# Fluorine in Silicon: Diffusion, Trapping, and Precipitation

X. D. Pi, C. P. Burrows, and P. G. Coleman[*]
*Department of Physics, University of Bath, Bath BA2 7AY, United Kingdom*

(Received 16 December 2002; published 17 April 2003)

The effect of vacancies on the behavior of F in crystalline Si has been elucidated experimentally for the first time. With positron annihilation spectroscopy and secondary ion mass spectroscopy, we find that F retards recombination between vacancies ($V$) and interstitials ($I$) because $V$ and $I$ trap F to form complexes. F diffuses in the $V$-rich region via a vacancy mechanism with an activation energy of 2.12 ± 0.08 eV. After a long annealing time at 700 °C, F precipitates have been observed by cross-section transmission electron microscopy which are developed from the $V$-type defects around the implantation range and the $I$-type defects at the end of range.

DOI: 10.1103/PhysRevLett.90.155901 PACS numbers: 66.30.Jt, 61.72.Tt

An incomplete picture of the basic behavior of F in Si blocks the realization of its full potential in microelectronic technology, although it has been incorporated in Si in several device processes [1–3]. The incorporation of F is usually realized by ion implantation. The threshold dose of F to amorphize Si is $10^{15}$ cm$^{-2}$. F is mobile only above 550 °C in both crystalline and amorphized Si. A strong surface-oriented diffusion has been observed in the former and, in the latter, F additionally accumulates at the amorphous-crystalline interface and in the extended interstitial($I$)-type defects beyond the amorphous layer [4,5]. By implanting high-dose BF$_2$ to obtain a region of high-density interstitials at the end of range (EOR) of implantation, Park *et al.* [6] proposed an interstitialcy mechanism of F diffusion with an activation energy ($E_m$) of 0.16 eV; this small $E_m$ implies transient diffusion of simple $I$-F complexes. However, to date no unambiguous evidence has been gathered to demonstrate the effect on F diffusion of the other kind of damage induced by implantation, the vacancy ($V$). Szeles *et al.* [7] studied this using positron annihilation spectroscopy (PAS) [8]. However, no convincing model was presented because the low densities of F in their samples gave no measurable PAS signature.

In this Letter, implantation of F at high energy (0.5 MeV) and dose ($5 \times 10^{15}$ cm$^{-2}$) produced a large number of vacancies in a wide region below the surface, separated from the $I$-rich region at EOR [9,10], so that the effect of implantation-induced defects on F could be studied. Implantation of $\langle 100 \rangle$ Czochralski (Cz) Si (P doped, 2–4 $\Omega$ cm) was carried out at a tilt of 7° at room temperature at the University of Surrey Ion Beam Center. The implanted samples were heated in vacuum by electron beam bombardment at 400 and 700 °C, being below and above the previously suggested critical temperature for F diffusion, for times ranging from 30 s to 125 h. Beam-based PAS and secondary ion mass spectroscopy (SIMS) were used to measure the as-implanted and heated samples. The as-implanted sample and that heated at 700 °C for 125 h were examined by cross-section transmission electron microscopy (XTEM). XTEM showed that the as-implanted sample remained crystalline although the dose was higher than the threshold value previously reported; this is due to the high implantation energy used here.

Figure 1 shows the PAS results for the as-implanted sample and those annealed at (a) 400 °C for up to 67 h and (b) 700 °C for up to 125 h. The trapping of positrons

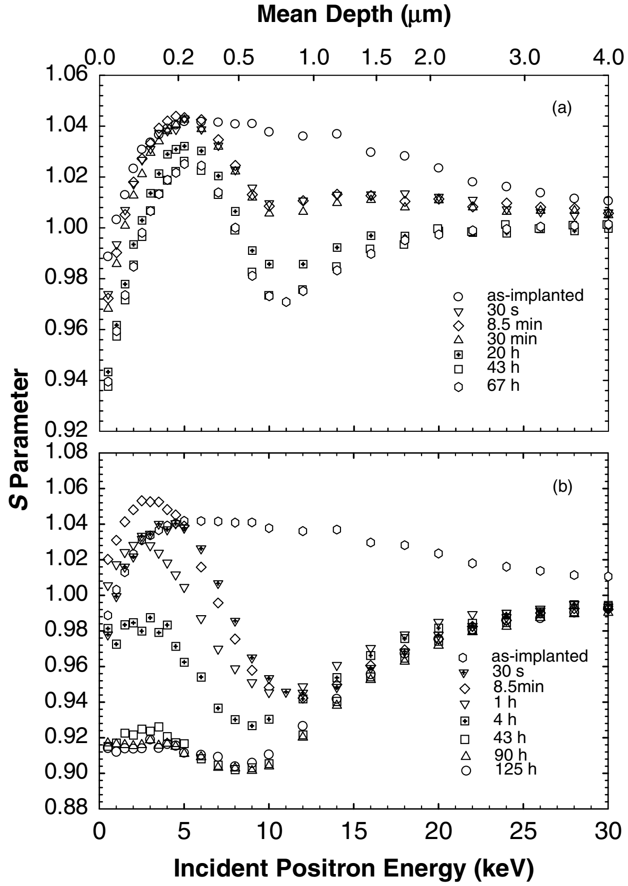

FIG. 1. PAS results for the samples annealed at (a) 400 °C for up to 67 h and (b) 700 °C for up to 125 h.

0031-9007/03/90(15)/155901(4)$20.00

at $V$-type defects leads to a higher Doppler-broadened line-shape parameter $S$ defined as the central fraction of the annihilation line, compared with that for the defect-free lattice sites. The $S$ values presented here have been normalized with respect to that for a bulk virgin Si sample for which $S$ is thus 1. The mean depth sampled by implanted positrons is determined by their incident energy $E$ (keV) and is $\sim 17E^{1.6}$ (nm). Figure 2 shows the F profiles in the as-implanted and annealed samples measured by SIMS. The implantation range ($R_p$) of 0.5 MeV F is $\sim$0.9 $\mu$m. By fitting the PAS data using VEPFIT [11], we find that the vacancy distribution ends at around 2.3 $\mu$m; such an abnormally deep distribution of vacancies has been observed previously [12]. It is believed that F atoms react with interstitials effectively during ion implantation; this allows the survival of most of the vacancies, which can then migrate over long distances.

The peak value of $S$ in the as-implanted sample is 1.042, characteristic of the divacancy ($V_2$) with our PAS setup [13]. It is reproducibly found that a dip appears around 11 keV (Fig. 1) in the $S$ curve for the as-implanted sample, which corresponds to the region close to $R_p$. It is well known that F and O reduce $S$ when they are associated with vacancies because of the large momenta of their outermost-shell electrons [14–16]. We also find that the gamma ray spectrum of our F as-implanted Si measured at $\sim$11 keV is unique compared with other ion implantations including O (not presented here). Therefore, we conclude that F has already decorated some vacancies around $R_p$ because of the high F concentration there.

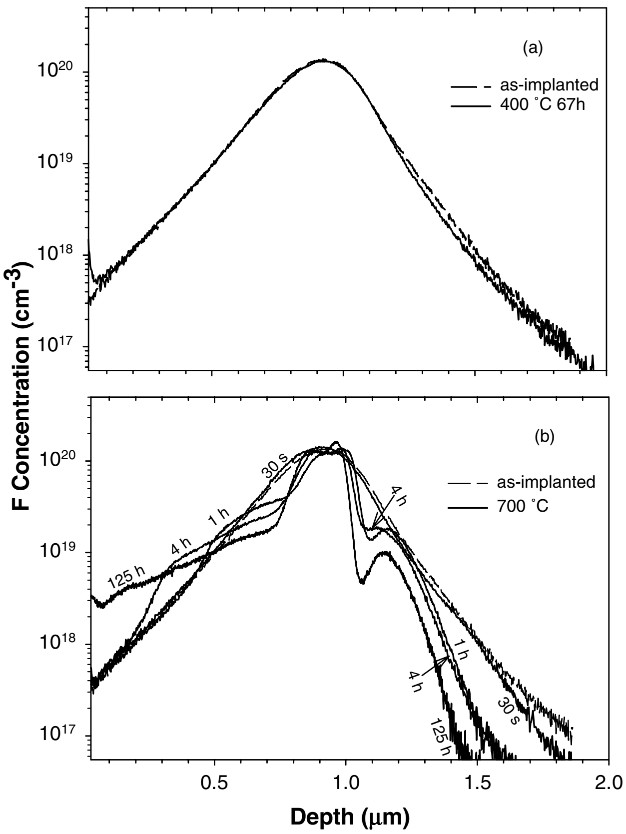

FIG. 2. F profiles measured by SIMS in the as-implanted sample and those annealed at (a) 400 and (b) 700 °C.

Figure 3 shows the changes in general $S$ obtained by fitting the data of Fig. 1(a) in regions I (0–0.5 $\mu$m), II (0.5–1.1 $\mu$m), and III (1.1–1.8 $\mu$m) with time at 400 °C until equilibrium is reached after 43 h. It is interesting that there are still vacancies in the region beyond $R_p$ although there is shrinkage from 2.3 to 1.8 $\mu$m during heating. SIMS shows that the F concentration is much less than $10^{18}$ cm$^{-3}$ beyond 1.8 $\mu$m in the as-implanted sample [Fig. 2(a)]. This low concentration facilitates $V$-$I$ recombination ($I$ being mainly in the form of $I$-F complexes) rather than the formation of $V$-F complexes.

The formation of $V$-F complexes in region II is evidenced by the clear decrease of $S$ (Fig. 3). In contrast, the $S$ values in regions I and III increase to be between 1.046 and 1.057, characteristic of trivacancy ($V_3$) and quadrivacancy ($V_4$), respectively, in the first 8.5 min. The dominance of vacancy agglomeration up to the size of $V_4$ is a consequence of the lower F concentration in these two regions [Fig. 2(a)]. After 8.5 min, the $S$ values in regions I and III begin to decrease. It is known that defect agglomeration usually proceeds via Ostwald ripening [17], in which dissociated components from small defects move to big ones to make them bigger. We believe that some of the dissociated vacancies can be lost to the surface from region I and to the bulk from region III. The effect of the loss of vacancies outweighs that of the increase of defect size, and so $S$ decreases in these two regions after 8.5 min. Because of the high implantation energy, the vacancy distribution can be regarded as uniform in the $V$-rich region [18], and a $V_2$ concentration of $\sim 8.5 \times 10^{18}$ cm$^{-3}$ in the region $\leq 1.1$ $\mu$m can be estimated with VEPFIT from PAS in the as-implanted sample. It is clear that the F concentration is higher than the

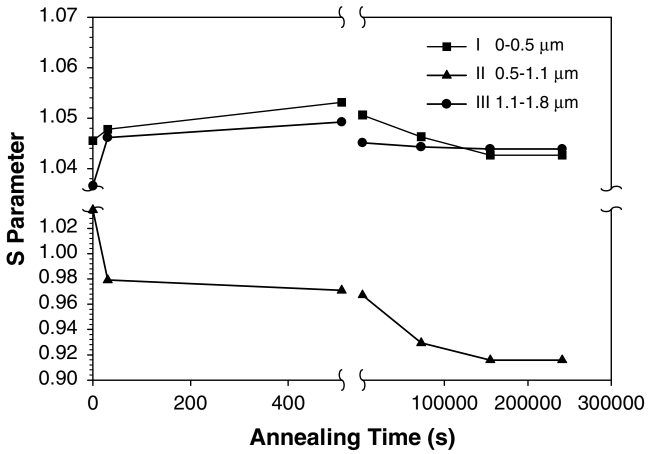

FIG. 3. The change of general $S$ values obtained from VEPFIT in different regions during annealing at 400 °C. The error bars are smaller than the symbols. The solid lines are used to guide the eye.

vacancy concentration in region II. We believe that F-dominated $V$-F complexes are produced so that the $S$ value becomes smaller than 1 after a long annealing time. In region I, however, $V$-dominated $V$-F complexes are formed. Hence, the $S$ value in this region is always larger than 1. Region III is $I$ rich because it is well beyond $R_p$; it is supposed that some isolated F is left after the formation of $I$-F complexes in this region in the as-implanted sample and that this initiates the formation of $V$-dominated $V$-F complexes, outcompeting the $V$-$I$ reaction ($I$ being mainly in $I$-F complexes) at 400 °C. $S$ is thus still larger than 1 even after a long annealing time. The existence of $V$-F complexes in region III again implies that F can prevent $V$-$I$ recombination by forming complexes.

Figure 2(a) shows that after 67 h annealing at 400 °C the F concentration below $\sim$1.1 $\mu$m is appreciably unchanged, consistent with the earlier observations that implanted F does not diffuse below 550 °C. This apparently contradicts the PAS results described above, i.e., that F migrates to form $V$-F complexes. $E_m$ values of 0.6–1.6 eV for interstitial F [19] and 1.3 eV for $V_2$ [20] mean that they both can diffuse at 400 °C. However, they trap each other to form $V$-F complexes once they meet. In region II, for example, the F concentration is $\sim 10^{20}$ cm$^{-3}$ and the mean distance between F and $V_2$ is estimated as 2.4 nm. It is considered that F travels less than this distance to react with $V_2$. This is a quick stage, illustrated by the significant decrease in $S$ after the first 30 s annealing at 400 °C [Figs. 1(a) and 3]. After that, the agglomeration of $V$-F complexes takes place slowly via Ostwald ripening, and $S$ changes very slowly with time in region II. The distance traveled by the simple $V$-F complex lies between 2 and 5 nm. The best depth resolution of modern SIMS is $\sim$3 nm (more generally 10 nm) [21], and so it is not able in this case to demonstrate F migration at 400 °C. Assuming a random walk mechanism, we estimate that $E_m$ for simple $V$-F complexes is $2.12 \pm 0.08$ eV with the expression $N = \nu t \exp(-E_m/kT)$, where $N$ is the jump number given by $(R/d)^2$ ($R$ is the diffusion distance and $d$ is 0.23 nm, the nearest neighbor distance in Si), $\nu$ is the Debye frequency ( $\sim 10^{13}$ Hz), and $t$ is the migration time (43 h). It is clear that F diffuses in the $V$-rich region in the form of simple $V$-F complexes, i.e., via a vacancy mechanism, although the higher $E_m$ of these $V$-F complexes makes F less mobile than in the interstitial state.

It is seen in Fig. 2(a) that the F concentration beyond $\sim$1.1 $\mu$m decreases somewhat after 67 h annealing at 400 °C. In region III simple $I$-F complexes, which are formed either in the as-implanted sample or during the Ostwald ripening of $I$-type defects, diffuse into the bulk to cause the F concentration to decrease.

The PAS results for annealing at 700 °C for up to 125 h are shown in Fig. 1(b). After 30 s it is found from VEPFIT that the $V$-type defects disappear in the region beyond $\sim$1 $\mu$m. This is a more significant shrinkage than at 400 °C, suggesting that $V$-$I$ recombination is significantly enhanced at 700 °C even though a comparatively high F concentration exists.

After 30 s annealing, a large decrease of $S$ appears at about 11 keV. VEPFIT shows that the general $S$ in the region from 0.5 to 1 $\mu$m becomes smaller than its equilibrium value in this region after annealing at 400 °C. This implies significant formation of advanced F-dominated $V$-F complexes in this region. F can travel farther at 700 °C than at 400 °C, and the change of F profile is clearly seen by SIMS. In the region shallower than 0.5 $\mu$m, however, $S$ increases and, as in the initial stage of annealing at 400 °C, $V_2$ agglomerate up to the size of $V_4$.

After 8.5 min annealing at 700 °C, the shallow region is shown by VEPFIT to contract to $\sim$0.4 $\mu$m and its $S$ increases to between 1.057 and 1.068, characteristic of $V_4$ and $V_5$, respectively, suggesting that the defects up to the size of $V_5$ are formed. With time the agglomerates grow and the vacancy density decreases in an Ostwald ripening process. $S$ in the shallow region decreases although there is no change in F concentration after 1 h annealing. The $S$ value for the shallow region would not become smaller than 1 if only vacancies were lost. F migrating from around $R_p$ introduces a further decrease in $S$. Therefore, the widening of the region with a low $S$ is observed, which is illustrated by the motion of the dip of $S$ curve from the original $\sim$11 to $\sim$8 keV after 43 h annealing [Fig. 1(b)]. It is seen in Fig. 1(b) that after 90 h there is no more change in the $S$ curve and F ceases to migrate (otherwise, $S$ would continue to decrease to be at least the value seen at $E \sim 7$ keV). The Ostwald ripening of agglomerates in the shallow region is also thought to be completed at 90 h. The flat part of $S$ curve after 90 h corresponds to the first $\sim$0.4 $\mu$m in the sample. This is consistent with the rather uniform distribution of vacancies in the shallow region and the small F concentration gradient there after a long annealing time [Fig. 2(b)].

Figure 4 shows the XTEM image of the sample annealed at 700 °C for 125 h. It is clear that there are two bands of F precipitates formed in this sample whose locations are consistent with those of two main SIMS F

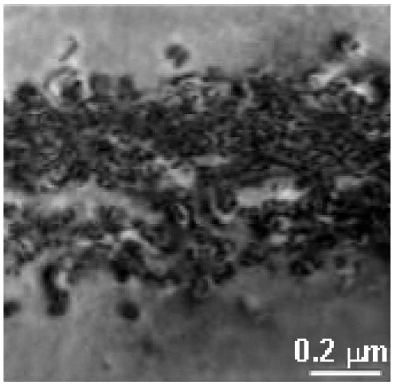

FIG. 4. XTEM image of the annealed F-implanted Si (700 °C, 125 h). The upper limit of F precipitates is at 0.75 $\mu$m depth.

peaks shown in Fig. 2(b). F precipitates can be developed from both $V$- and $I$-type defects. $V$-F complexes formed around $R_p$ (0.75–1 $\mu$m) can act as the nuclei of F precipitates. The other F peak, in the $I$-rich region from 1–1.3 $\mu$m, appears after only 1 h annealing. Extended $I$-type defects such as {311} are generated at EOR at 700 °C [22], and these serve as the nuclei of F precipitates. Between the two bands of F precipitates, the numbers of $V$ and $I$ are closely matched, so that during annealing mutual annihilation leaves very few $V$- or $I$-type defects to act as the nuclei of F precipitates.

The F concentration beyond ~1 $\mu$m decreases with time during annealing at 700 °C [Fig. 2(b)]. {311} defect formation is also a process of Ostwald ripening, in which dissociated simple $I$-F complexes diffuse quickly into the bulk. The extended $I$-type defects act as nuclei for F precipitates. Fast-diffusing $I$-F complexes can also be released during the formation of F precipitates to relax the stress, analogous to the formation of O precipitates [23].

Compared with the decrease of F concentration in the area where F precipitates are developed from $I$-type defects, the increase of F concentration around 0.95 $\mu$m after 125 h annealing [Fig. 2(b)] indicates that $V$-type defects attract F atoms much more effectively than $I$-type defects as nuclei of F precipitates. Vacancies can reduce the stress induced by the formation of F precipitates so that it is easier for them to grow from $V$-type defects. This also explains why, in addition to the initially higher F concentration, there is a much higher density of F precipitates in the band between 0.75 and 1 $\mu$m (Fig. 4).

Although vacancies can help relax stress during F precipitation, interstitials may still be emitted in this process. It is found in Fig. 2(b) that there is a loss of F (e.g., ~20% after 4 h) in the $V$-rich region before 90 h at 700 °C. The increase of F concentration in the formation area of F precipitates cannot account for all of the loss. We consider that a part of the lost F diffuses out of the surface in the form of simple $I$-F complexes, in which interstitials are emitted from F precipitates developed from $V$-type defects. Owing to the transient diffusion of simple $I$-F complexes, no change of F concentration is induced in the near-surface region.

The story of F diffusion in the $V$-rich region at 700 °C is clearly different from that described above. It is seen in Fig. 2(b) that, in addition to migrating to F precipitates at ~0.95 $\mu$m, F diffuses from the high-concentration region near $R_p$ towards the surface, consistent with the change of $S$ shown in Fig. 1(b). As at 400 °C, we obtain that $E_m$ of F in the $V$-rich region is 2.19 eV, assuming F at 0.9 $\mu$m takes 90 h to reach the surface; this falls into the range obtained before, leading to the conclusion that F also diffuses via a vacancy mechanism here.

The absence of defects seen by XTEM at <0.75 $\mu$m means that the defects inducing the low $S$ values in this region are $V$-F clusters whose sizes are below the threshold of XTEM visibility.

In summary, F retards $V$-$I$ recombination in Si. F diffuses in the $V$-rich region via a vacancy mechanism. The loss of F in the $I$-rich region and a part of that in the $V$-rich region can be explained by the transient diffusion of simple $I$-F complexes. After a long annealing time at 700 °C, F precipitates are developed from both $V$- and $I$-type defects. It is hoped that the basic insights gained here will contribute materially to the development of useful F-related structures.

This work is supported by EPSRC Grants No. GR/M51895 and No. GR/M54001. H. Perrott and Professor R. Stevens helped us with XTEM. SIMS was performed by MATS UK.

---

*Electronic address: p.g.coleman@bath.ac.uk

[1] D. F. Downey, C. M. Osburn, and S. D. Marcus, Solid State Technol. **40**, 71 (1997).
[2] J. D. Williams and P. Ashburn, J. Appl. Phys. **72**, 3169 (1992).
[3] T. P. Ma, J. Vac. Sci. Technol. A **10**, 705 (1992).
[4] M. Y. Tsai *et al.*, J. Appl. Phys. **50**, 188 (1979).
[5] S. P. Jeng *et al.*, Appl. Phys. Lett. **61**, 1310 (1992).
[6] Y. J. Park and J. J. Kim, J. Appl. Phys. **85**, 803 (1999).
[7] C. Szeles *et al.*, J. Appl. Phys. **76**, 3403 (1994).
[8] *Positron Beams*, edited by P. G. Coleman (World Scientific, Singapore, 2000).
[9] B. Nielson *et al.*, J. Appl. Phys. **74**, 1636 (1993).
[10] O. W. Holland *et al.*, J. Electron. Mater. **25**, 99 (1996).
[11] A. van Veen *et al.*, in *Analysis of Positron Profiling Data by Means of "VEPFIT"*, AIP Conf. Proc. No. 218 (AIP, New York, 1990), p. 171.
[12] M. Fujinami and N. B. Chilton, J. Appl. Phys. **73**, 3242 (1993).
[13] X. D. Pi, C. P. Burrows, and P. G. Coleman, Appl. Surf. Sci. **194**, 255 (2002).
[14] A. Uedono *et al.*, Jpn. J. Appl. Phys. Pt. 1 **36**, 2571 (1997).
[15] P. G. Coleman, N. B. Chilton, and J. A. Baker, J. Phys. Condens. Matter **2**, 9355 (1990).
[16] M. Fujinami, Phys. Rev. B **53**, 13 047 (1996).
[17] W. Ostwald, Z. Phys. Chem., Stoechiom. Verwandtschaftsl. **34**, 495 (1900).
[18] P. G. Coleman, C. P. Burrows, and A. P. Knights, Appl. Phys. Lett. **80**, 947 (2002).
[19] A. Taguchi and Y. Hirayama, Solid State Commun. **116**, 595 (2000).
[20] G. D. Watkins and J. W. Corbett, Phys. Rev. **138**, A543 (1965).
[21] *Growth and Characterisation of Semiconductors*, edited by R. A. Stradling and P. C. Klipstein (Adam Hilger, Bristol, 1990).
[22] S. Coffa, S. Libertino, and C. Spinella, Appl. Phys. Lett. **76**, 321 (2000).
[23] U. Gösele and D. G. Ast, Technical Report No. DOE/JPL/956046-83/9 (DE40009494), U.S. Department of Energy, 1983.